Daily adaptive proton therapy: Is it appropriate to use analytical dose calculations for plan adaption?

L Nenoff[†1,2], M Matter[1,2], A G Jarhall[1,9,10], C Winterhalter[1,2], J Gorgisyan[1,3], M Josipovic[4], G F Persson[4,5,6], P Munck af Rosenschold[9,10], D C Weber[1,7,8], A J Lomax[1,2], F Albertini[1]

[1]*Paul Scherrer Institute, Center for Proton Therapy, Switzerland*

[2]*Department of Physics, ETH Zurich, Switzerland*

[3]*Institute of Radiation Physics, Lausanne University Hospital, Lausanne, Switzerland*

[4]*Department of Oncology, Rigshospitalet Copenhagen University Hospital, Denmark*

[5]*Department of Oncology, Herlev-Gentofte Hospital Copenhagen University Hospital, Denmark*

[6]*Department of Clinical Medicine, Faculty of Medical Sciences, University of Copenhagen, Denmark*

[7]*Department of Radiation Oncology, University Hospital Zurich, Switzerland*

[8]*Department of Radiation Oncology, University Hospital Bern, Switzerland*

[9]*Radiation Physics, Department of Hematology, Oncology and Radiation Physics, Skåne University Hospital, Lund, Sweden*

[10]*Medical Radiation Physics, Lund University, Lund, Sweden*

Corresponding author: Lena Nenoff

lena.nenoff@psi.ch

Paul Scherrer Institute, WBBB 105, 5232 Villigen PSI, Switzerland

bullet points: proton therapy, adaptive therapy, monte carlo, analytical dose calculation

Abstract

Purpose: The accuracy of analytical dose calculations (ADC) and dose uncertainties resulting from anatomical changes are both limiting factors in proton therapy. For the latter, rapid plan adaption is necessary, whereas for the former, Monte Carlo (MC) approaches are instead being increasingly recommended. These however are inherently slower than analytical approaches, potentially limiting the ability to rapidly adapt plans. Here, we compare the clinical relevance of uncertainties resulting from both.

Materials and Methods: Five non-small-cell lung cancer (NSCLC) patients with up to nine CTs acquired during treatment and five paranasal (HN) patients with 10 simulated anatomical changes (sinus filling), were analyzed. On the initial planning-CTs, treatment plans were optimized and calculated using an ADC and then recalculated with MC. Additionally, all plans were recalculated (non-adapted) and re-optimized (adapted), on each repeated CT using the same ADC as for the initial plan and resulting dose distributions compared.

Results: When comparing analytical and MC calculations in the initial treatment plan and averaged over all patients, 94.2% (NSCLC) and 98.5% (HN) of voxels had differences <±5% and only minor differences in CTV V95 (average <2%) were observed. In contrast, when re-calculating nominal plans on the repeat (anatomically changed) CTs, CTV V95 degraded by up to 34%. Plan adaption however restored CTV V95 differences between adapted and nominal plans to <0.5%. Adapted OAR doses remained the same or improved.

Conclusion: Dose degradations caused by anatomical changes are substantially larger than uncertainties introduced by the use of analytical instead of MC dose calculations. Thus, if the use of analytical calculations can enable more rapid and efficient plan adaption than MC approaches, they can, and indeed should be used for plan adaption for these patient groups.

Introduction

High dose conformity and steep dose gradients can be achieved with proton therapy, allowing for excellent normal tissue sparing (1, 2). This makes proton therapy especially suitable for pediatric cancer or for tumors close to organs at risk, including tumors in the brain, head and neck (HN) and lung, and clinical benefits were shown (3–10).

However, the large density heterogeneities between air/lung, bone and soft tissue in these anatomical regions are known to be difficult to model with analytical dose calculations. As such, Monte Carlo (MC) dose calculations are increasingly being recommended (11, 12), particularly in regions with complex density heterogeneities as observed in the lung and around the nasal cavities (13–16). Additionally, a number of studies have reported shortcomings of some analytical algorithms when a range shifter is used (17, 18) although this has not been observed for other analytical algorithms (19).

On the other hand, anatomical changes can also substantially limit the accuracy of proton therapy. These also frequently occur in HN (20, 21) and lung cancer patients (22, 23) and can cause large dose distortions during the treatment course. Thus, regular plan adaption is advised in these areas (24–26).

To deal with slow anatomical changes, such as weight gain or loss, it is sufficient to adapt the plan within a few days (27). However, other changes, such as rectal, bladder or nasal cavity filling, should be adapted as quickly as possible, ideally on a daily basis, and within a short time (e.g. 5-10 minutes) after daily imaging. Previous studies have shown that adapting the plan on the daily anatomy has advantages over using anatomically robust optimization (26). Current adaption protocols are however time and resource consuming. Times required for re-planning using MC optimization, which take 5 minutes or more at best, are incompatible with daily online adaption and a high throughput patient workflow (28,29). Re-planning using an analytical algorithm on the other hand can be extremely time efficient, reducing the complete re-planning process to just a few seconds (30), enabling rapid plan adaption on a daily basis.

In this study therefore, we investigate whether an online adaptive protocol based on plan re-optimization using a fast, but limited accuracy analytical algorithm can still provide improvements to the overall treatment dose for patients with cancer in the lung and HN regions. For this, we compare dose differences to the nominal plan as a result of anatomical changes to those arising from the use of an analytical dose calculation, and contrast these to those resulting if an online adaptive approach is used.

Materials and Methods

Patient data and treatment plans

Five NSCLC patients (previously treated with photon radiotherapy), and 5 patients treated with protons in the paranasal region were included in this study (Figure 1a). All NSCLC patients had locally advanced tumors including mediastinal lymph nodes and showed large anatomical variations during treatment. To mitigate intra-fractional motion in the lung cases, voluntary, visually guided deep-inspiration breath-hold (DIBH) was used for all CTs. During the treatment course, up to 9 additional DIBH CTs were acquired (31), referred to as repeat CTs. An intensity modulated proton therapy (IMPT) plan consisting of 3 individually selected fields was calculated for each patient on the initial DIBH planning CT (Figure 1b) using a prescribed dose of 66 Gy (RBE) in 2Gy (RBE) per fraction (32) (RBE = 1.1 (33)).

For the paranasal tumor patients, artificially generated CTs were used, as described elsewhere (25), simulating 10 CTs during the treatment course (referred to as simulated CTs), each with random anatomy and setup differences. Anatomical changes were simulated by filling each pre-contoured nasal cavity independently by first overwriting with the HU of air, and then with the HU of mucus in a layer-wise approach (26) with a randomly selected filling stage (25). The layer-wise approach was considered to most realistically mimic actual filling of the nasal cavities (26) and with a random filling selected for each daily delivery, a worst case scenario has been simulated. For all paranasal cases, 4-field IMPT plan was optimized to deliver 60 Gy (RBE) in 30 fractions (Figure 1b).

All cases have been planned and optimized using a clinically validated and in-house developed analytical algorithm (34), which scales dose calculation grid points to their water equivalent depth in the patient (based on CT information) and approximates lateral scatter using a single Gaussian model. Airgaps are considered by using different look-up tables for the beamsize in air, which is given by the moments of the angular spatial distribution and depending on nozzle extraction, preabsorber setting and beam

energy, together with a contribution due to multiple Coulomb scattering based on the water equivalent depths of the calculation point (34). This algorithm has recently been implemented on GPU hardware and has been shown to be able to fully re-optimise complete treatment plans in just a few seconds (30).

Monte Carlo simulations

All initial plans were recalculated using the TOPAS MC tool (35), using the default physics libraries and tuned to model beam data from PSI Gantry 2 (19, 36). The number of protons per pencil beam in the MC simulations were calculated directly from the number of protons provided by the treatment planning system, divided by 1000. This results in statistical fluctuations of less than 1% (37). Each MC field was normalized to the same mean PTV dose as the corresponding analytical field (19). After this, all MC fields were summed up to construct the MC recalculated plan (Figure 1c).

Structures and fraction dose during treatment

For the NSCLC patients, all repeat CTs (Figure 1d) were first aligned to the planning CT using rigid image registration (RIR) to propagate the target contours, and then with deformable image registration (DIR) for OAR contour propagation using Velocity (Varian Medical Systems, Palo Alto, USA). OAR contours were visually verified and corrected as necessary. As the anatomical changes of paranasal patients were directly simulated in the planning CT, no image registration was necessary and all structures were rigidly propagated. For all patients, treatment plans were recalculated (non-adapted) and re-optimized (online adapted) on all repeat CTs using the same ray casting (analytical) algorithm and input parameters as for the initial treatment plan on the planning CT (Figure 1e and f). Additionally, for one NSCLC patient all DAPT plans were also recalculated with MC.

Evaluation methods

3% and 5% voxel specific dose differences for all voxels with dose >10% of the prescribed dose between the analytical and MC dose distributions were evaluated, excluding dose in air. Also, differences between dose parameters for the CTV (D98, V95) and selected OARs for doses calculated on the on-treatment CTs were evaluated for all cases.

Results

Differences between analytical and Monte Carlo dose calculations

For both NSCLC and paranasal tumor patients, voxel specific agreement between the analytical and MC dose distributions was good, with more than 94.2% and 98.5% of the voxels on average having differences <±5% respectively. However, this higher voxel dose agreement for paranasal tumor patients compared to NSCLC patients did not translate into a better agreement between OARs. Indeed, differences in OARs and, as expected, in the CTV V95, D98 doses were similar for both treatment sites (Table 1a).

Effect of anatomical changes.

For all patients, plans were recalculated (non-adapted) and re-optimized (adapted) on all repeated and simulated CTs with the ADC. Differences in CTV coverage and in the dose to selected organs at risks (OARs) are shown in Figures 2 and 3, respectively.

For non-adapted plans, the CTV V95 is severely degraded (Table 1b), resulting in a reduction compared to the initial plan of -2.8% [ranging from -5.2% to -2.1%] and of -15% [-34.5% to -0.9%] for NSCLC and paranasal patients respectively. However, plan adaption could restore the CTV coverage (mean difference between reoptimized and initial CTV V95 < 0.5%, Table 1c, Figure 2 and 3) and, in some cases, could even improve coverage compared to the initial plan (e.g. the D98% was increased by 1.9% with adaption for NSCLC patient 5).

Similar results were observed for OAR sparing, with the mean heart dose for the NSCLC cases increasing by up to 3.3% [2.1% - 5.4%] (NSCLC patient 3) due to anatomical changes during treatment. The mean heart doses could, however, be restored to <0.6% of those of the nominal plan by using adaption. Lung dose did not change substantially with adaption, mainly due to the selection of beam angles from a plan robustness perspective and the lack of additional lung constraints in the re-optimization process. For the paranasal tumor patients, differences for single fraction doses to the chiasm (up to 5%, patient 1) and brainstem (up to 18.6%, patient 4) were observed, while DAPT substantially reduced these differences.

Finally, as the adapted plans have been calculated using the ADC only, we also recalculated the DAPT plans of NSCLC patient 4, the patient with the lowest agreement between MC and ADC in the initial plan using MC. The voxel-wise dose differences of more than 3% and 5% were on average 85.8% and 94.8% respectively, so in the range of those for the initial NSCLC plans shown in Table 1a.

Discussion

We have investigated the dose-effects of anatomical changes on proton therapy treatments in the lung and paranasal regions, and compared these to uncertainties resulting from using a fast analytical, rather than MC calculation engine. We have demonstrated that dose variations caused by anatomical changes are in general much larger than those caused by using the analytical rather than MC algorithm, particularly in relation to CTV coverage. As such, we could show that online analytical plan adaption, which restores the plan quality back to that of the nominal plan, is a valid approach to improve the overall treatment dose.

For both paranasal tumor and NSCLC patients, we found good agreement between our ADC and MC, with more than 94.2% and 98.5% of the voxels on average having differences of less than +/-5% respectively. This is in agreement with previous work from our group comparing these two algorithms (19), but in contrast to other publications performing similar comparisons with other analytical algorithms, where it has been suggested that such algorithms should be avoided in the presence of highly heterogeneous anatomies (14). However, even though in this study the NSCLC patients had rather

large tumor volumes (which implied less heterogeneity than for those investigated in (14)), the good agreement between analytical and MC for the majority of patients reported in this paper indicates that such algorithms can still be applicable for the fast adaption of proton treatments

In contrast, for both NSCLC and paranasal tumor patients, the dose quality was substantially degraded. Indeed, CTV V95% averaged over all repeated and simulated CTs, was reduced by up to 5.2% and 34.5% for NSCLC and HN patients respectively (Figure 2, Figure 3, Table 1b). The use of adaption restored CTV coverage almost completely in all cases and for all CTs (mean differences <0.5%). Interestingly, adaption has also been shown, in some cases, to improve dose to OARs (Figure 3). For example, note the drastic reduction of mean heart dose (averaged over all repeated CTs) of NSCLC patient 3 from +3.3% without adaption to -0.6% with adaption compared to the initial plan. As the heart dose is a predictor of overall survival for NSCLC patients (38) such an increase might have an effect on the patient outcome, depending on the initial heart dose.

In this study the anatomical changes for paranasal tumor patients have been generated by simulating nasal cavity fillings. This model assumes rather drastic interfractional anatomical changes, but has already been used in other studies (25, 26) and showed to provide a reasonable estimation of the effect of the fillings of the sinus. For the NSCLC patients on the other hand, clinically observed anatomical changes based on DIBH CTs acquired during the treatment course have been used. Previous studies evaluating NSCLC patients have reported suboptimal treatment doses in free-breathing mode, especially with large breathing motion (39), while DIBH (40) is an appropriate method to apply the proton dose safely to the patients (41). It has also been reported that inter-fractional anatomical changes cause larger dose distortions than breathing motion (22). This shows that for NSCLC patients, inter-fractional anatomical changes are challenging and that these patients could benefit from fast plan adaption, even if other sources of uncertainty still exist (e.g. the use of an analytical calculation for speed or breathing motion).

We have recalculated and adapted plans on each DIBH CT, thus assuming the whole treatment can then be applied within a single breath hold. In clinical practice a dose delivery for NSCLC patients takes typically 2-3 breathholds. We assume that a daily adaption would account for interfractional changes, while the visually guided breath-hold will mitigate intrafractional motion. Although this is a simplified approach, it is sufficient for our study in order to compare the effects of interfractional anatomical changes to those caused by analytical calculation approximations. In addition, we focused on the effects caused by anatomical changes to the dose distribution on each CT, which corresponds to a single fraction, whereas the dose deterioration would be reduced if the effect of fractionation was considered. Nevertheless, when the fraction effect was considered, a target dose degradation of more than 5% was reported for 3 out of 15 NSCLC patients and for 4 out of 5 HN patients (25, 32), indicating that adaption is necessary even if fractionation is considered.

It should be noted however, that doses in the repeat CTs (both non-adapted and adapted scenarios) have also been calculated with ADC rather than MC. Only for NSCLC patient 4 (the patient with the worst agreement between MC and ADC for the initial plan) the DAPT plans were also recalculated with MC. Dose differences between the two algorithms were similar as for the initial NSCLC plans (Table 1a)

and in agreement with previous publications (19). Indeed, they were even slightly better than the agreements found in the initial plan for this patient. In addition, the voxel-to-voxel agreement between analytical and MC was similar for all patients of each indication when comparing these calculation approaches on the nominal anatomy. As such, there is no reason to believe that differences between analytical and MC would be substantially different on the repeat, rather than planning CT's, and will therefore be substantially smaller than the difference observed due to anatomical changes.

We are aware that a fast plan optimization with MC would be preferable. However, even though recent developments achieved large improvements for the speed of proton MC dose calculations (29, 42–44), a full plan optimization takes ~5 minutes and is therefore still much slower than analytical approaches, which only take some seconds (30). In an on-line daily adaptive approach the calculation time is a critical factor, therefore for this application an ultra-fast analytical approach is preferable. Given that there are other potentially time-consuming processes that would also need to be performed as part of a daily adaptive approach, such as contour propagation and plan specific quality assurance (45), it is particularly important that the plan adaption/re-optimization is as fast as possible (29, 30). This currently can be best achieved using analytical calculations, even if their accuracy is somewhat compromised in comparison to a full Monte Carlo approach. However, as demonstrated, such differences are much smaller than those resulting from anatomical changes. In addition, MC calculations can also be incorporated into an analytical based DAPT workflow. For instance, after delivery of each adapted fraction, a full MC dose reconstruction could be performed on the anatomy of the day, by also taking into account information from the log-files of the delivered treatment (37). Such a log-file based MC dose calculation could then be used for offline QA and dose accumulation. Indeed, this is the approach that will be taken at our institute for the incorporation of a full MC-based dose calculation into the DAPT workflow. However, for dose accumulation deformable image registration might introduce additional not well quantifiable uncertainties (46–48). Alternatively, if a fast MC dose calculation (e.g. less than one minute) is available, a MC recalculation of the analytically optimized plan could also be performed as a QA measure directly before the delivery of the plan.

Conclusion

Dose uncertainties for NSCLC and paranasal patients caused by anatomical changes are substantially larger than those caused by the use of a simple, but fast, analytical dose calculation. We therefore caution the overuse of MC calculations for adaptive planning if the resulting time overhead compromises the ability to rapidly adapt treatment plans to anatomical changes.

Acknowledgments

We acknowledge the Swiss national science foundation [grant project: 320030 165961] for their support.

Tables

Table 1: a) Mean and range of differences in target coverage and voxel-dose-agreement (VDA) between the reference plan calculated on the initial CT with ADC and the dose re-calculated with MC. Differences are caused only by the algorithm. b) Mean and range of differences in target coverage and in selected OAR doses between the reference plan (calculated on the initial CT with ADC) and the plans re-calculated (with ADC) on all repeated and simulated CTs. Only differences caused by anatomical changes are considered. c) Mean and range of differences in target coverage and selected OAR doses between the reference plan (initial CT, ADC) and the plans re-optimized (adapted) on all repeated and simulated CTs.

		mean difference	
		NSCLC patients	paranasal patients
a) ADC vs MC	3% VDA	84.3 [82.6 - 86.7]	93.5 [91.1 - 95.0]
	5%VDA	94.2 [93.1 - 95.4]	98.5 [97.7 - 99.0]
	ΔCTV V95	-1.1 [-4.9 - 0.8]	-1.6 [-3.1 - -0.3]
	ΔCTV D98	-1.2 [-4.0 - 0.2]	-1.5 [-3.5 - -0.2]
	Δheart mean	0.1 [-0.4 - 0.7]	
	ΔV20 lung	2.3 [0.4 - 4.4]	
	ΔV40 lung	0.2 [0.0 - 0.5]	
	ΔD2 brainstem		1.0 [0.5 - 2.0]
	ΔD2 chiasma		0.8 [0.2 - 1.4]
b) non-adapt	ΔCTV V95	-2.8 [-5.2 - -0.2]	-15.3 [-34.5 - -0.9]
	ΔCTV D98	-3.1 [-6.2 - -0.4]	-10.8 [-22.0 - -0.4]
	Δheart mean	1.3 [0.5 - 3.3]	
	ΔV20 lung	2.2 [-1.2 - 9.3]	
	ΔV40 lung	1.0 [-1.0 - 3.1]	
	ΔD2 brainstem		-1.0 [-3.8 - -0.2]
	ΔD2 chiasma		-1.0 [-1.8 - -0.1]
c) adapt	ΔCTV V95	0.5 [-0.1 - 1.1]	-0.3 [-0.7 - 0.0]
	ΔCTV D98	1.2 [-0.3 - 1.9]	-0.2 [-0.8 - 0.2]
	Δheart mean	0.3 [-0.6 - 1.2]	
	ΔV20 lung	2.5 [-9.6 - 3.7]	
	ΔV40 lung	-0.2 [-1.6 - 2.7]	
	ΔD2 brainstem		-0.4 [-1.9 - 0.7]
	ΔD2 chiasma		-0.1 [-1.9 - -0.1]

Figures

Figure 1:

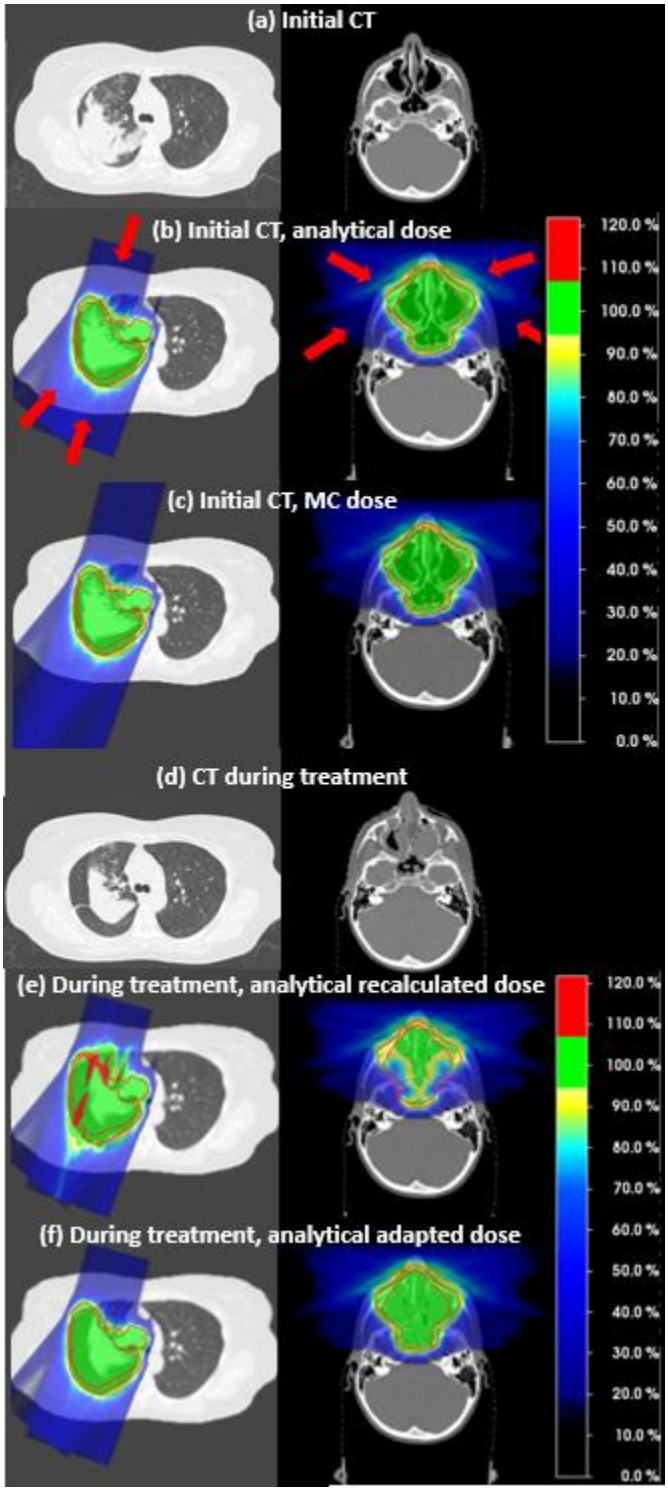

Figure 2:

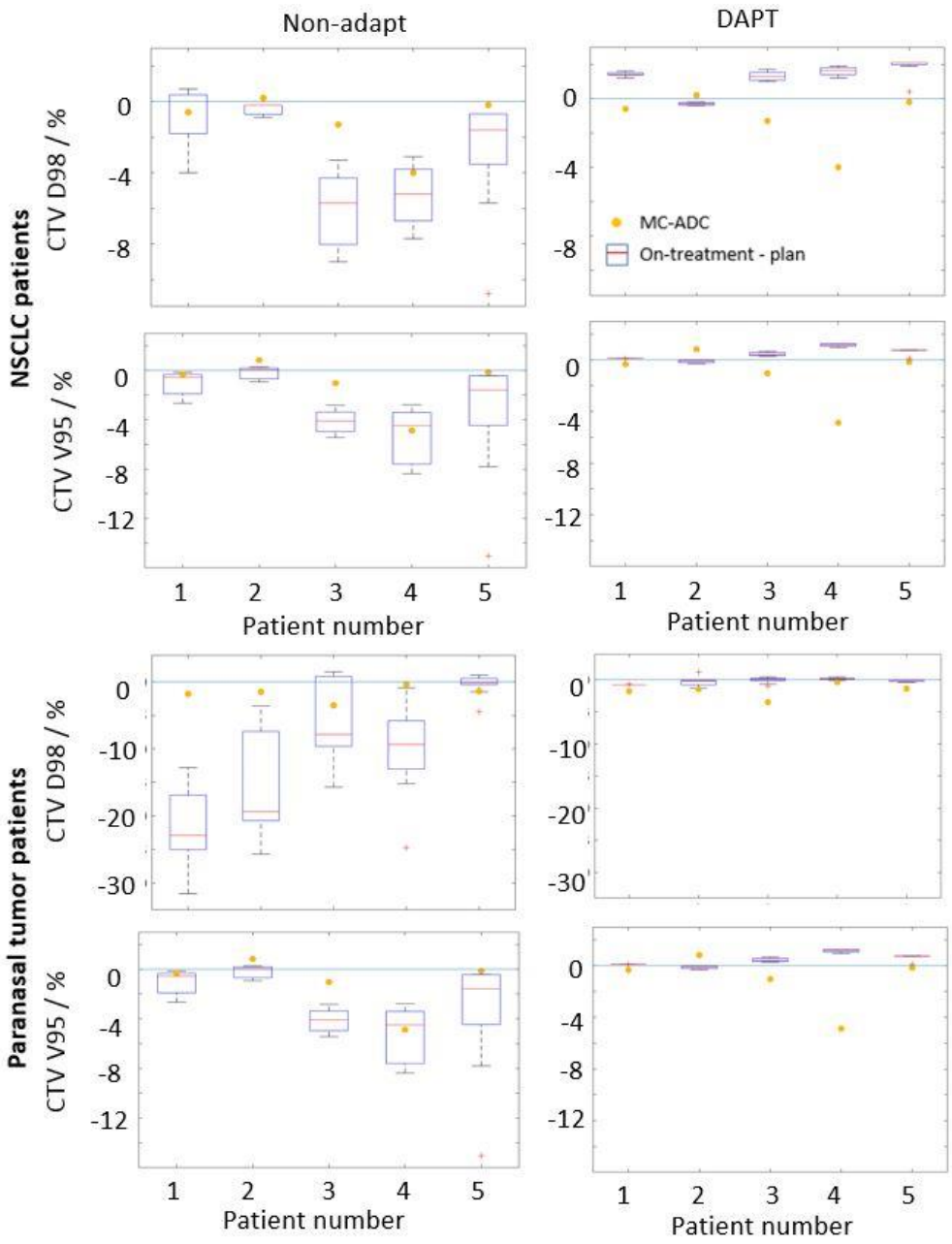
Non-adapt
DAPT
NSCLC patients
Paranasal tumor patients
CTV D98 / %
CTV V95 / %
MC-ADC
On-treatment - plan
Patient number

Figure 3:

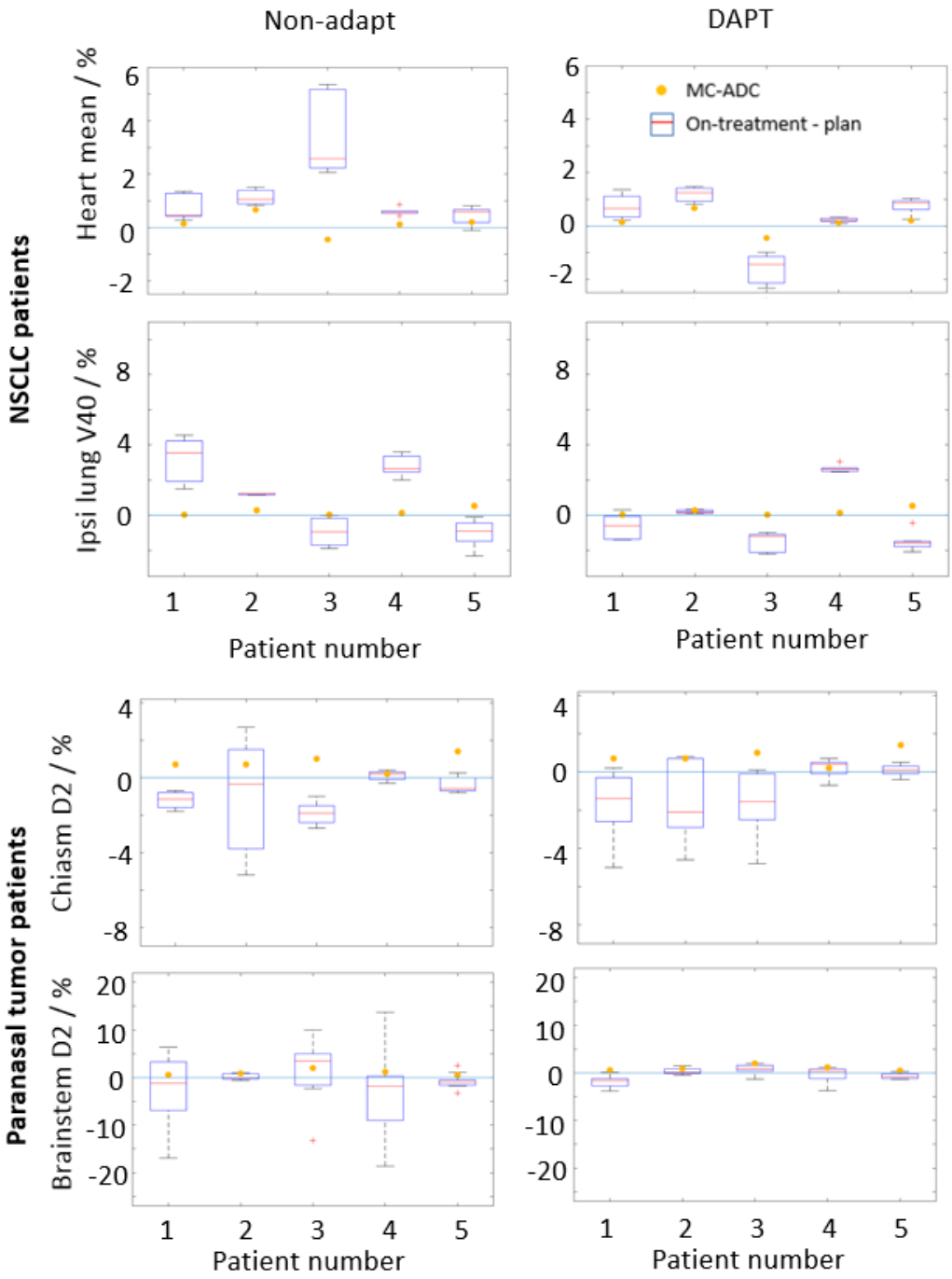
Non-adapt
DAPT
NSCLC patients
Heart mean / %
Ipsi lung V40 / %
MC-ADC
On-treatment - plan
Patient number
Paranasal tumor patients
Chiasm D2 / %
Brainstem D2 / %
Patient number

Figure captions

Figure 1: Dose distributions for an example NSCLC and a paranasal tumor patient (a) calculated with an ADC on the initial planning CT, (b) recalculated on the initial CT with a MC algorithm, (c) recalculated (non-adapted,) on the repeated (NSCLC) or simulated (HN) CT and (d) reoptimized (adapted) on the repeated or simulated CT. Field directions, CTV and PTV contour are shown in red.

Figure 2: The effect of anatomical changes in relation to the effect of dose algorithm on CTV coverage for NSCLC and paranasal patients: Differences relative to the dose optimized with ADC on the initial planning CT due to anatomical changes are shown in boxes, differences between MC and ADC on the initial plan with yellow circles. If plans are not adapted (left) differences caused by the algorithm are smaller or similar than caused by anatomy. Adaption (right) reduces dose differences due to anatomy changes to a smaller or similar level as the difference in algorithm. Boxes show median, 25% and 75% percentile, whiskers the most extreme data points within 1.5 interquartile range, outliers more extreme than this are marked with +.

Figure 3: The effect of anatomical changes in relation to the effect of dose algorithm for selected OARs. The difference relative to the dose optimized with ADC on the initial planning CT due to anatomical changes are shown in boxes, differences between MC and RC on the initial plan with yellow circles. Differences due to the algorithm are smaller or similar than differences due to anatomy (left). Adaption (right) reduces dose differences due to anatomy. Boxes show median, 25% and 75% percentile, whiskers the most extreme data points within 1.5 interquartile range, outliers more extreme than this are marked with +.

1. Hill-Kayser CE, Both S, Tochner Z, *et al.* Proton therapy: ever shifting sands and the opportunities and obligations within. 2011.

2. Baumann M, Krause M, Overgaard J, *et al.* Radiation oncology in the era of precision medicine. *Nat. Rev. Cancer*. 2016.

3. Nguyen Q-N, Ly NB, Komaki R, *et al.* Long-term outcomes after proton therapy, with concurrent chemotherapy, for stage II–III inoperable non-small cell lung cancer. *Radiother. Oncol.* 2015;115:367–372.

4. Pehlivan B, Ares C, Lomax AJ, *et al.* Temporal lobe toxicity analysis after proton radiation therapy for skull base tumors. *Int. J. Radiat. Oncol. Biol. Phys.* 2012;83:1432–40.

5. Weber DC, Badiyan S, Malyapa R, *et al.* Long-term outcomes and prognostic factors of skull-base chondrosarcoma patients treated with pencil-beam scanning proton therapy at the Paul Scherrer Institute. *Neuro. Oncol.* 2016;18:236–43.

6. Weber DC, Rutz HP, Pedroni ES, *et al.* Results of spot-scanning proton radiation therapy for chordoma and chondrosarcoma of the skull base: The Paul Scherrer Institut experience. *Int. J. Radiat. Oncol. Biol. Phys.* 2005;63:401–409.

7. Weber DC, Schneider R, Goitein G, *et al.* Spot Scanning-Based Proton Therapy for Intracranial Meningioma: Long-Term Results From the Paul Scherrer Institute. *Int. J. Radiat. Oncol.* 2012;83:865–871.

8. Mendenhall NP, Malyapa RS, Su Z, *et al.* Proton therapy for head and neck cancer: Rationale, potential indications, practical considerations, and current clinical evidence. *Acta Oncol. (Madr).* 2011;50:763–771.

9. Holliday EB, Frank SJ. Proton Radiation Therapy for Head and Neck Cancer: A Review of the Clinical Experience to Date. *Int. J. Radiat. Oncol.* 2014;89:292–302.

10. Holliday EB, Garden AS, Rosenthal DI, *et al.* Proton Therapy Reduces Treatment-Related Toxicities for Patients with Nasopharyngeal Cancer: A Case-Match Control Study of Intensity-Modulated Proton Therapy and Intensity-Modulated Photon Therapy. *Int. J. Part. Ther.* 2015;2:19–28.

11. Saini J, Traneus E, Maes D, *et al.* Advanced Proton Beam Dosimetry Part I: review and performance evaluation of dose calculation algorithms. *Transl. lung cancer Res.* 2018;7:171–179.

12. Schuemann J, Dowdell S, Grassberger C, *et al.* Site-specific range uncertainties caused by dose calculation algorithms for proton therapy. *Phys. Med. Biol.* 2014;59:4007–31.

13. Grassberger C, Daartz J, Dowdell S, *et al.* Quantification of proton dose calculation accuracy in the lung. *Int. J. Radiat. Oncol. Biol. Phys.* 2014.

14. Taylor PA, Kry SF, Followill DS. Pencil Beam Algorithms Are Unsuitable for Proton Dose Calculations in Lung. *Int. J. Radiat. Oncol. Biol. Phys.* 2017.

15. Schuemann J, Giantsoudi D, Grassberger C, *et al.* Assessing the Clinical Impact of Approximations in Analytical Dose Calculations for Proton Therapy. *Int. J. Radiat. Oncol. Biol. Phys.* 2015.

16. Maes D, Saini J, Zeng J, *et al.* Advanced proton beam dosimetry part II: Monte Carlo vs. pencil beam-

based planning for lung cancer. *Transl. lung cancer Res.* 2018;7:114–121.

17. Widesott L, Lorentini S, Fracchiolla F, *et al.* Improvements in pencil beam scanning proton therapy dose calculation accuracy in brain tumor cases with a commercial Monte Carlo algorithm. *Phys. Med. Biol.* 2018;63:145016.

18. Saini J, Maes D, Egan A, *et al.* Dosimetric evaluation of a commercial proton spot scanning Monte-Carlo dose algorithm: comparisons against measurements and simulations. *Phys. Med. Biol.* 2017;62:7659–7681.

19. Winterhalter C, Zepter S, Shim S, *et al.* Evaluation of the ray-casting analytical algorithm for pencil beam scanning proton therapy. *Phys. Med. Biol.* 2019;64:065021.

20. Kraan A, Van de Water S, Teguh D, *et al.* Dose Uncertainties in IMPT for Oropharyngeal Cancer in the Presence of Anatomical, Setup and Range Errors. In: *Medical Physics*.; 2012.

21. Stützer K, Jakobi A, Bandurska-Luque A, *et al.* Potential proton and photon dose degradation in advanced head and neck cancer patients by intratherapy changes. *J. Appl. Clin. Med. Phys.* 2017;18:104–113.

22. Szeto YZ, Witte MG, van Kranen SR, *et al.* Effects of anatomical changes on pencil beam scanning proton plans in locally advanced NSCLC patients. *Radiother. Oncol.* 2016;120:286–292.

23. Harada H, Murayama S. Proton beam therapy in non-small cell lung cancer: state of the art. *Dovepress*. 2017;8:141–145.

24. Bernatowicz K, Geets X, Barragan A, *et al.* Feasibility of online IMPT adaptation using fast, automatic and robust dose restoration. *Phys. Med. Biol.* 2018;63:085018.

25. Nenoff L, Matter M, Hedlund Lindmar J, *et al.* Daily Adaptive Proton Therapy: the key to use innovative planning approaches for paranasal cancer treatments. *Acta Oncol. (Madr).* 2019;63:085018.

26. Van De Water S, Albertini F, Weber DC, *et al.* Anatomical robust optimization to account for nasal cavity filling variation during intensity- modulated proton therapy : a comparison with conventional and adaptive planning strategies. *Phys. Med. Biol.* 2018;63:11–22.

27. Albertini F, Bolsi A, Lomax AJ, *et al.* Sensitivity of intensity modulated proton therapy plans to changes in patient weight. *Radiother. Oncol.* 2008;86:187–194.

28. Ma J, Beltran C, Seum H, *et al.* A GPU-accelerated and Monte Carlo-based intensity modulated proton therapy optimization system. 2014.

29. Botas P, Kim J, Winey B, *et al.* Online adaption approaches for intensity modulated proton therapy for head and neck patients based on cone beam CTs and Monte Carlo simulations. *Phys. Med. Biol.* 2018;64:015004.

30. Matter M, Nenoff L, Meier G, *et al.* IMPT plan generation in under ten seconds on a GPU. *Acta Oncol. (Madr).* 2019.

31. Josipovic M, Persson GF, Dueck J, *et al.* Geometric uncertainties in voluntary deep inspiration breath hold radiotherapy for locally advanced lung cancer. *Radiother. Oncol.* 2016;118:510–514.

32. Gorgisyan J, Munck af Rosenschold P, Perrin R, *et al.* Feasibility of Pencil Beam Scanned Intensity Modulated Proton Therapy in Breath-hold for Locally Advanced Non-Small Cell Lung Cancer. *Int. J. Radiat. Oncol.* 2017;99:1121–1128.

33. Paganetti H. Relative biological effectiveness (RBE) values for proton beam therapy. Variations as a function of biological endpoint, dose, and linear energy transfer. *Phys. Med. Biol.* 2014;59.

34. Schaffner B, Pedroni E, Lomax A. Dose calculation models for proton treatment planning using a dynamic beam delivery system: an attempt to include density heterogeneity effects in the analytical dose calculation. *Phys. Med. Biol.* 1999;44:27–41.

35. Perl J, Shin J, Schümann J, *et al.* TOPAS: An innovative proton Monte Carlo platform for research and clinical applications. *Med. Phys.* 2012;39:6818–6837.

36. Winterhalter C, Fura E, Tian Y, *et al.* Validating a Monte Carlo approach to absolute dose quality assurance for proton pencil beam scanning. *Phys. Med. Biol.* 2018;63.

37. Winterhalter C, Meier G, Oxley D, *et al.* Log file based Monte Carlo calculations for proton pencil beam scanning therapy. *Phys. Med. Biol.* 2019;64:035014.

38. Speirs CK, DeWees TA, Rehman S, *et al.* Heart Dose Is an Independent Dosimetric Predictor of Overall Survival in Locally Advanced Non–Small Cell Lung Cancer. *J. Thorac. Oncol.* 2017;12:293–301.

39. Jakobi A, Perrin R, Knopf A, *et al.* Feasibility of proton pencil beam scanning treatment of free-breathing lung cancer patients. *Acta Oncol. (Madr).* 2018;57:203–210.

40. Boda-Heggemann J, Knopf A-C, Simeonova-Chergou A, *et al.* Deep Inspiration Breath Hold—Based Radiation Therapy: A Clinical Review. *Int. J. Radiat. Oncol.* 2016;94:478–492.

41. Dueck J, Knopf A-C, Lomax A, *et al.* Robustness of the Voluntary Breath-Hold Approach for the Treatment of Peripheral Lung Tumors Using Hypofractionated Pencil Beam Scanning Proton Therapy. *Int. J. Radiat. Oncol.* 2016;95:534–541.

42. Jia X, Schümann J, Paganetti H, *et al.* GPU-based fast Monte Carlo dose calculation for proton therapy. *Phys. Med. Biol.* 2012;57:7783–7797.

43. Schiavi A, Senzacqua M, Pioli S, *et al.* Fred: a GPU-accelerated fast-Monte Carlo code for rapid treatment plan recalculation in ion beam therapy. *Phys. Med. Biol.* 2017;62:7482–7504.

44. Senzacqua M, Schiavi A, Patera V, *et al.* A fast - Monte Carlo toolkit on GPU for treatment plan dose recalculation in proton therapy. *J. Phys. Conf. Ser.* 2017;905:012027.

45. Matter M, Nenoff L, Meier G, *et al.* Alternatives to patient specific verification measurements in proton therapy: a comparative experimental study with intentional errors. *Phys. Med. Biol*. 2018.

46. Sonke J-J, Belderbos J. Adaptive Radiotherapy for Lung Cancer. *Semin. Radiat. Oncol.* 2010;20:94–106.

47. Zhang L, Wang Z, Shi C, *et al.* The impact of robustness of deformable image registration on contour propagation and dose accumulation for head and neck adaptive radiotherapy. *J. Appl. Clin. Med. Phys.* 2018;19:185–194.

48. Miura H, Ozawa S, Nakao M, *et al.* Impact of deformable image registration accuracy on thoracic images with different regularization weight parameter settings. *Phys. Medica*. 2017;42:108–111.